Available online at www.sciencedirect.com
SCIENCE DIRECT®
International Journal of Heat and Mass Transfer 48 (2005) 1808–1818
International Journal of HEAT and MASS TRANSFER
www.elsevier.com/locate/ijhmt

Gas bubble dynamics—experiment and fractal analysis

J.T. Cieslinski [a], R. Mosdorf [b,*]

[a] Gdansk University of Technology, Narutowicza 11/12, 80-952 Gdansk, Poland
[b] Bialystok University of Technology, Wiejska 45, 15-351 Bialystok, Poland

Received 10 November 2004
Available online 22 January 2005

Abstract

In the paper, nonlinear features of the air bubbling from a submerged glass nozzles are discussed. The air bubbles were emitted from glass nozzles of different diameters submerged in distilled water at a depth of 15 cm in a cylindrical tank of 30 cm in diameter and 37 cm height. The air volume flow rate was changed from 1 l/h to 45 l/h. A laser-photodiode and an acoustic technique system have been used. Also photographic study of bubbles departure has been carried out. Measured data have been analysed using the fractal analysis method. It has been shown that bubbles dynamics is of deterministic chaos nature and behaviours of such system can be chaotic or periodic depending on the volume flow rate. The map of chaos appearance has been constructed. Data recorded by acoustic system has been used to analysis of bubble wall movement.

Keywords: Bubble dynamics; Nonlinear analysis

1. Introduction

The knowledge of bubble dynamics is of key importance in physical, biological and medical processes, and particularly in industrial applications such as aeration, fermentation, saturation, homogenisation, degassing, fluidization, smelting, froth flotation, boiling, etc. Despite of numerous experimental and theoretical investigations the reliable model even for the most simple case of single bubble formation still remains a formidable task.

A variety of systems for effecting gas–liquid contacting have been studied experimentally. The injection devices used vary from simple orifices, nozzles, capillaries, holes (sonic holes) and slots to multiple orifice plates or even porous (sintered) disks. The complexity of the process is enormous. There are numerous system and physical parameters including physical properties of the two phases, gas flow rate, pressure above nozzle or orifice plate, height of the liquid, gravity conditions which exert varying levels of influence on the formation of bubbles. Hence, most of the efforts have been devoted to the formation of bubbles from single nozzles or orifice plates [1–7], among the others. In the present study air bubbles were generated on artificial site formed by glass nozzle into a stagnant water.

Investigation of bubble formation and sizing in laboratory experiments has relied on high-speed photography [8], application of an electrical triple probe [9] or novel video techniques [10,11]. In recent years several laser techniques have been developed for simultaneous measurements of bubble velocity and size. Among the latter are holography [12], the phase-Doppler method [13], tomography [14], the Schlieren technique [15], and Particle Image Velocimetry technique [16–18]. The emission of an acoustic signal by bubbles on formation and deformation is well known [19]. According to [20] "the

* Corresponding author. Tel./fax: +48 85 7422 393.
E-mail address: mosdorf@ii.pb.bialystok.pl (R. Mosdorf).

0017-9310/$ - see front matter © 2005 Elsevier Ltd. All rights reserved.
doi:10.1016/j.ijheatmasstransfer.2004.12.002

Nomenclature

C	correlation integral
d	nozzle diameter, distance in phase space in Eqs. (1) and (2)
D	correlation dimension
f	mean frequency, 1/s
Fr	Froude number; $Fr = \frac{w_o^2}{gd}$
N	number of samples
P	amplitude of subsequent frequencies of Fourier series
q	parameter
St	Strouhal number; $St = \frac{fd}{w_o}$
t	time, s
V	volume flow rate
We	Weber number; $We = \frac{\rho_l d w_o^2}{\sigma}$
w_o	outlet air velocity
X	measured value

Greek symbols

Θ	Heviside's step function
σ	surface tension
τ	time interval, s

Subscripts

i, j	sample number
d	departure
l	liquid

initial drop in the acoustic signal pressure is due to the contraction of the tip of the bubble during the neck-breaking process. The peak in acoustic signal pressure is caused by a jet of liquid that penetrates the bubble after neck breaking—[21]". In [22] an acoustic technique coupled with high-resolution photographs for bubble sizing has been applied.

Numerous modelling studies have been conducted on the bubble formation from a single orifice or nozzle submerged in liquids [5,23–26], among the others. The basis of many theoretical models is in the assumption that the bubble is spherical and by application of a force balance acting on the bubble due to the main effects of buoyancy, surface tension, gas momentum effects and liquid inertia effects the motion of the bubble can be predicted. Most lately, in [27] the comprehensive model has been presented that takes into account instantaneous interactions between successive bubbles as well as incorporates the wake effect of previous bubble. Furthermore, it is known that the volume of the gas chamber connected to the orifice (nozzle) is an important factor in determining the initial bubble size and frequency of bubble emission. Two limiting modes of bubble formation are distinguished: constant flow rate regime (CFRR) and constant pressure regime (CPR). The CFRR can be obtained by imposing a strong restriction between the settling chamber and the injection point, in such a way that the incoming flow of the bubble should be controlled and therefore constant. To achieve constant flow rate conditions a small diameter connection pipe between the gas bomb and the settling chamber or additional valve was applied, respectively [22,28]. In [29] the sonic hole of very small diameter (50 μm) was constructed. The CPR occurs whenever the chamber volume is sufficiently large (in practice > 1000 cc—[30]) and the pressure in the gas chamber is maintained constant. With progression of time and the extent of bubble formation, pressure drop across the orifice (nozzle) varies and thereby resulting in a non-constant flow rate. In [31] has been suggested that the bubbles are formed under CFRR provided that the orifice Reynolds number is larger than 1000, and CPR prevails for orifice Reynolds number smaller than 1000. Lately, it has been stated [29], that it is impossible to obtain a CFRR, even using a sonic hole.

According to [32] bubble motion and bubble shape are controlled by deterministic forces, such as body force and drag force caused by the convective motion, and the complex and non-linear input of the liquid motion including wake and turbulent motion surrounding the bubbles. Therefore new approaches based on fractal and deterministic chaos analyses have been applied to investigate the complex phenomena of multi-phase systems [33–35]. The concept of non-linear dynamics systems has also been applied to study chaotic features of gas bubbling from a single nozzle (orifice) [32,36–44].

In the present study the results of two experiments have been analyzed from the point of view of non linear dynamics of bubbles growth and departure. Experiment with laser-photodiode system has been used to obtain the time periods between the subsequent bubbles. The dependence of frequency of bubble departure on different internal diameter of nozzle and different volume flow rates has been found out. The hydrophone system has been used to analyze the dynamics of bubbles deformation after departure.

2. Experimental setup

2.1. Air supply system

The scheme of the experimental equipment is shown in Fig. 1. Air bubbles were emitted from glass nozzles submerged in distilled water at a depth of 15 cm in a

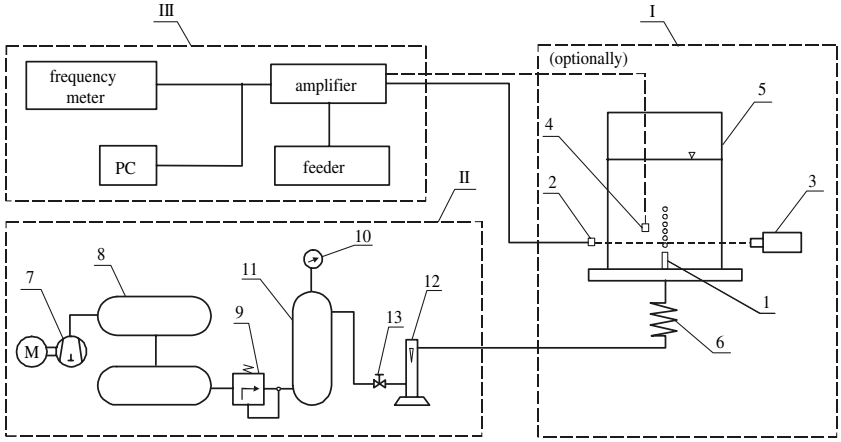

Fig. 1. Experimental equipment for gas bubbling. I: injection system (1: injection device, 2: photo-diode, 3: He–Ne laser, 4: hydrophone, 5: water tank, 6: capillary tube); II: air supply system (7: non-lubricant compressor, 8: air buffer reservoir, 9: pressure regulator, 10: manometer, 11: settling chamber, 12: rotameter, 13: needle valve); III: data acquisition system with audio card.

cylindrical tank of 30 cm in diameter and 37 cm height. The volume of the settling chamber was 0.03 m^3. The settling chamber is fed by air coming from a gas buffer reservoir through a pressure regulator and an individually calibrated rotameter accurate to ±1%. The air volume flow rate was changed from 1 l/h to 45 l/h. The pipe from the rotameter to the injection nozzle is a 2 mm inner diameter aluminium tube. The bubbles were produced in pressure-controlled mode. Experiments have been conducted for constant supply overpressure in the settling chamber (11 in Fig. 1). Individually calibrated manometer accurate to ±0.2% has been employed to measure overpressure in the settling chamber.

2.2. Laser-photodiode system

A laser-photodiode system coupled with a standard PC audio card to analyse bubble release frequency has been developed (Fig. 1). As a light source served Spindler & Hoyer diode laser (type DS670) of 1 mW output power and wave length of red light 670 nm. Spindler & Hoyer silicon photodiode E10V was utilised as a photo detector. The voltage output generated by photodiode was recorded at the frequency of 11 kHz. The 8 bit A/D converter was used to convert time series recorded into the series of time intervals (X) for further processing. The values of time series changed in the range 0–255. A typical sample size was 20,000 points.

Three glass nozzles of 0.75 mm, 1.61 mm and 2.76 mm in internal diameter and length equal to 55 mm have been investigated using laser-photodiode system with constant supply overpressure in the settling chamber of 40 kPa. External diameter of glass nozzle was adequately: 5.32 mm, 7.94 mm, 5.86 mm. The laser ray was located 8 mm above nozzle outlet (Fig. 2(c)).

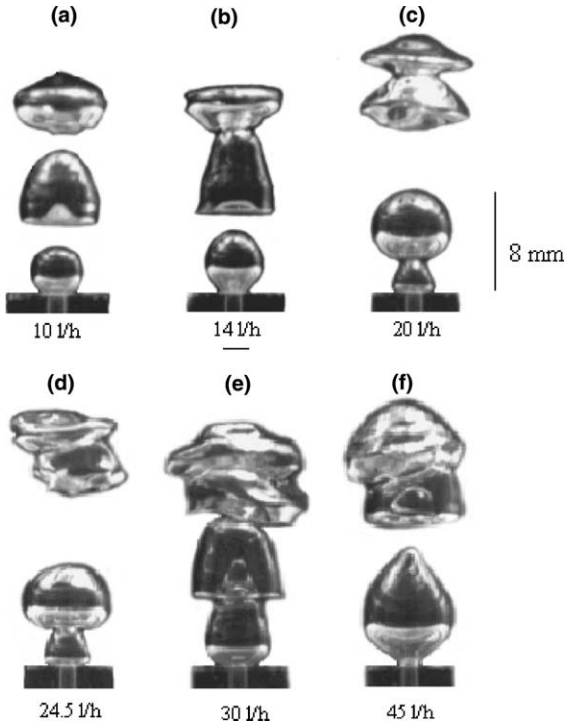

Fig. 2. Typical behaviour of bubble train versus volume flow rate for nozzle $d = 1.61$ mm and constant overpressure in the settling chamber $P = 40$ kPa.

2.3. Acoustic technique system

A hydrophone B&K 8105 was employed in order to record acoustic signal generated by departing bubbles. A hydrophone was placed 10 mm away from nozzle

outlet. Samples of voltage generated by microphone were recorded at the frequency of 11 kHz. The glass nozzle 0.9 mm in internal diameter, external diameter equal to 9.9 mm and length 57.5 mm has been used. The experiments have been conducted for constant supply overpressure in the settling chamber of 10 kPa.

2.4. Visualization instrumentation

A system based on flash lamp Hama SF-30E coupled with photographic camera Pentax ME Super equipped with converging lens has been developed in order to visualize gas bubbling.

3. Bubble behaviours

As an example in Fig. 2 typical sequence of bubble formation from the nozzle with outlet diameter of $d = 1.61$ mm and for different volume flow rates have been presented. The same flow structures were observed for all investigated nozzles. For low volume flow rate no coalescence of subsequent departing bubbles was observed, so the process of bubbles departure is periodic (Fig. 2(a)). For volume flow rate ca. 10 l/h, bubble coalescence commences as it is shown in Fig. 2(b). For high volume flow rate coalescence of bubbles takes place already on nozzle mouth (Fig. 2(c)–(e)). In this case time periods between the departing bubbles become irregular. For the highest volume flow rate applied slender detaching bubbles have been observed (Fig. 2(f)) due to rapid movement of the previous bubble.

Fig. 3 shows typical changes of measurement signal recorded by photodiode for different volume flow rates and different nozzle diameters with constant overpressure in the settling chamber. On the right side of Fig. 3(a) it has been schematically shown the dependence between the bubble location and signal level. The recorded signal reaches the lowest value for bubble crossing the laser ray at its maximum diameter. For free pass of laser beam through the gap between succeeding bubbles recorded signal value obtains the highest value. The method of release frequency detection based on laser-photodiode system can not be applied for volume flow rate higher than 14 l/h owing to coalescence of bubbles on nozzle mouth.

Detailed analysis of signal presented in Fig. 3 allows to differentiate two time intervals for low volume flow rate: one representing free pass of laser beam between succeeding bubbles τ_1 and second—τ_2 representing time of laser ray bubble crossing (Fig. 3(b)). The crossing time τ_2 is distinctly shorter than free pass interval τ_1. Both time intervals increase with nozzle diameter increase. Crossing time increase with nozzle diameter increase means increasing bubble departure diameter. Free pass interval increase means decreasing release

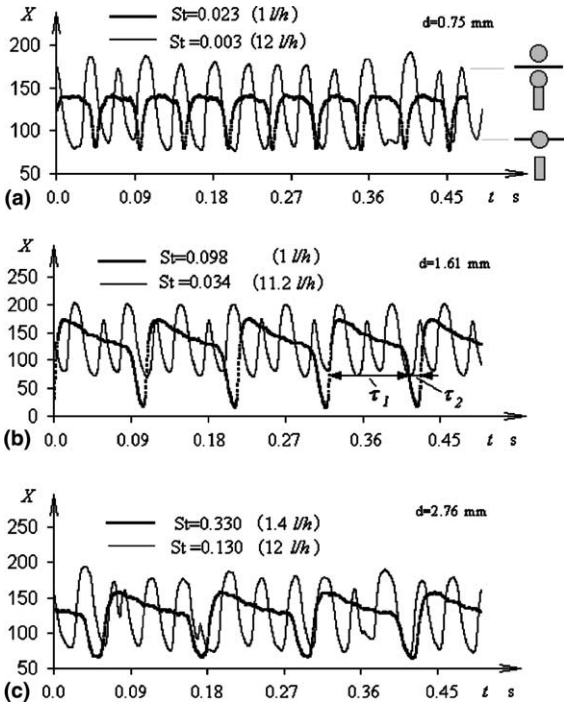

Fig. 3. Changes of signal recorded by laser-photodiode system for different volume flow rates and internal diameter of glass nozzles for overpressure in the settling chamber $P = 40$ kPa: (a) $d = 0.75$ mm, (b) $d = 1.61$ mm, (c) $d = 2.76$ mm.

bubble frequency. The results for low volume flow rate allow to draw following conclusion: increase in nozzle diameter leads to increasing departure diameter and decreasing release frequency.

For volume flow rate 12 l/h average bubble release frequency becomes independent on the nozzle diameter, but bubble formation process is still influenced by a nozzle diameter. The changes of signal are similar to periodic (Fig. 3(b)) and chaotic (Fig. 3(a) and (c)) ones. The results show that mean values of some parameters, such as mean release frequency are not sufficient to describe bubble dynamics and more detailed analysis is required.

In Fig. 4 typical changes of signal recorded by hydrophone for constant overpressure in settling chamber are displayed. Presented data correspond to acoustic signal generated by single bubble. Time of acoustic signal duration depends on volume flow rate, but signal courses seem to be similar (Fig. 4(a) and (b)).

Signals recorded by hydrophone are quite different from samples of voltage generated by photodiode (Fig. 3). This results from the different measurement techniques applied. In the case of laser-photodiode system, the signal course corresponds to location of a bubble passing through the laser ray. For acoustic measurement, according to [18], the greatest peak corresponds

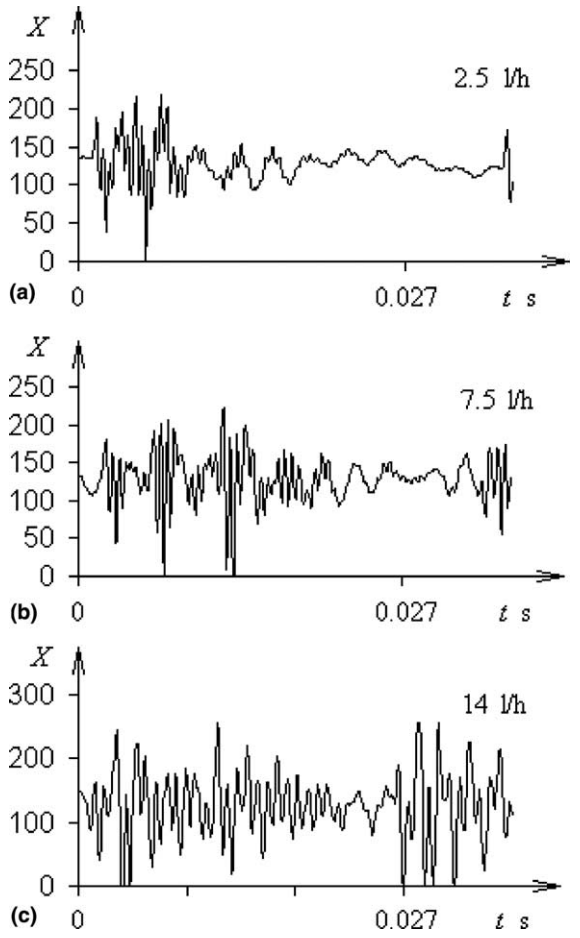

Fig. 4. Changes of acoustic signal recorded by hydrophone system for different volume flow rates and $d = 0.9$ mm for overpressure in the settling chamber $P = 10$ kPa: (a) $V = 2.5$ l/h, (b) $V = 7.5$ l/h, (c) $V = 14$ l/h.

to contraction of the tip of the bubble during the neck-breaking process. The signal changes between two succeeding peaks illustrate oscillations of the bubble due to compression of the air inside the bubble. This process is visible to some extent in Fig. 2. After bubble detachment, the bottom part of bubble rapidly moves up and becomes concave (Fig. 2(a) and (b)). This process generates the wave on bubble surface and changes the shape of departing bubble into the disc visible in Fig. 2(a) and (c). These two above mentioned processes influence the pressure changes recorded by hydrophone.

4. Data analysis and discussion

Non linear analysis starts from attractor reconstruction. The attractor reconstruction from the recorded data allows identification the nature of processes responsible for data generation. Reconstruction of attractor in certain embedding dimension has been carried out using the stroboscope coordination. In this method subsequent co-ordinates of attractor points are calculated basing on the subsequent samples distant of time delay τ. The time delay is multiplication of time between the samples.

The dimension spectrum D_q is one of the essential characteristics of attractors, and it allows identification the structure of attractors, especially the level of complexity of attractor versus attractor points density and is defined by the following expression [45]:

$$D_q = \lim_{l \to 0} \frac{1}{\ln d} \ln C^q(d) \tag{1}$$

where

$$C^q(d) = \left[\frac{1}{N} \sum_i \left(\frac{1}{N} \sum_j \Theta(d - | X_i - X_j |) \right)^{q-1} \right]^{1/q-1} \tag{2}$$

Θ Heaviside's step function that determines the number of attractor's point pairs of the distance shorter than d

q parameter

Parameter q indicates attractor points density for which the dimension is calculated. For $q \to -\infty$, D_q characterizes the part of attractor with low density of points. For $q \to +\infty$ dimension D_q characterizes the area of attractor with high density of points. For $q = 2$, D_q is called the correlation dimension [45–47].

Fig. 5 shows the 3D attractor reconstruction from data presented in Fig. 3. Attractors shown in Fig. 5(b) and (f) seem to be characteristic for chaotic system. Correlation dimension of attractors shown in Fig. 5(a), (c) and (e) depends on time delay and changes in the range between 2 and 3. Because of high level of noise in signal shown in Fig. 3(a) and (b) the proper estimation of correlation dimension is impossible. The correlation dimension of attractors, shown in Fig. 5(b) and (f) for embedding dimension equal to 20 is above 4.

Fig. 6 presents examples of time intervals between subsequent bubbles for different volume flow rate and nozzle diameters. Obtained results confirm that for low volume flow rate nozzle diameter increase results in increase of time interval between departing bubbles (Fig. 6(a)), while for high volume flow rate such kind of correlation does not occur (Fig. 6(b)).

Fig. 7 illustrates average release frequency of bubbles generated from submerged nozzle. For high volume flow rate the influence of nozzle diameter is much smaller than for low volume flow rate. Present data are in reasonable accord with data obtained by other researchers [2,5,48].

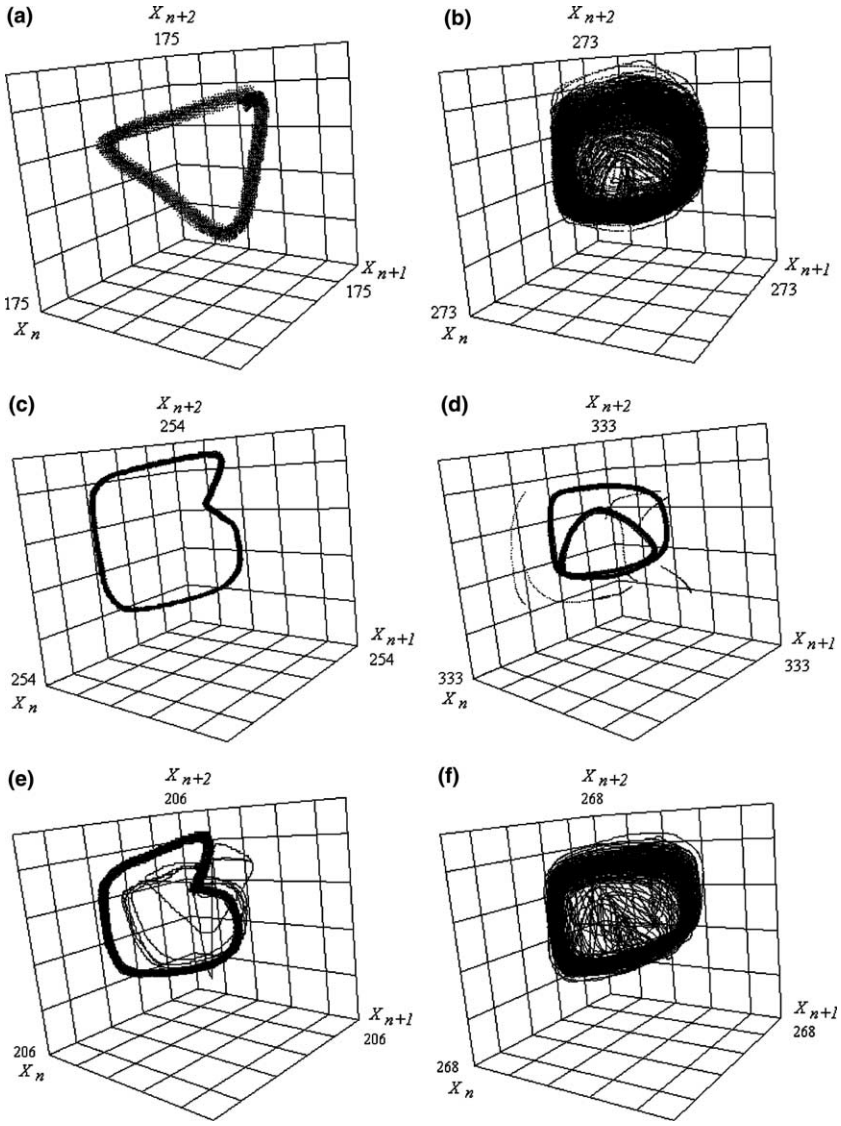

Fig. 5. 3D reconstruction of attractor for different volume flow rates and internal diameter of glass nozzles for overpressure in the settling chamber $P = 40$ kPa, $\tau = 0.0059$ s: (a) $d = 0.75$ mm, $St = 0.023$, $V = 1$ l/h; (b) $d = 0.75$ mm, $St = 0.003$, $V = 12$ l/h; (c) $d = 1.61$ mm, $St = 0.098$, $V = 1$ l/h; (d) $d = 1.61$ mm, $St = 0.034$, $V = 11.2$ l/h; (e) $d = 2.76$ mm, $St = 0.330$, $V = 1.4$ l/h; (f) $d = 2.76$ mm, $St = 0.130$, $V = 12$ l/h.

Presentation of experimental data with using the dimensionless numbers allows to obtain interesting information about bubbles behaviors. For instance, Fig. 8 shows present results in a dimensionless form as a function of Strouhal number St versus ratio of square Weber number to Froude number We^2/Fr. This parameter represents ratio of inertial forces to surface tension forces. For lower values of We^2/Fr Strouhal number is almost constant what indicates that release frequency is proportional to air volume flow rate. For higher values of We^2/Fr Strouhal number strongly decreases with increase of We^2/Fr value what means that release frequency does not depend on air volume flow rate.

Fig. 9 depicts the reconstruction of maps of chaos appearance in gas bubbling for different nozzle diameters and volume flow rates. Grey area indicates the region where the subsequent time intervals change chaotically. Black dots point out the observed value of time intervals. A single square for the given flow rate indicates that the process of bubbles departure is periodic. For the nozzle diameter equal to 2.76 mm

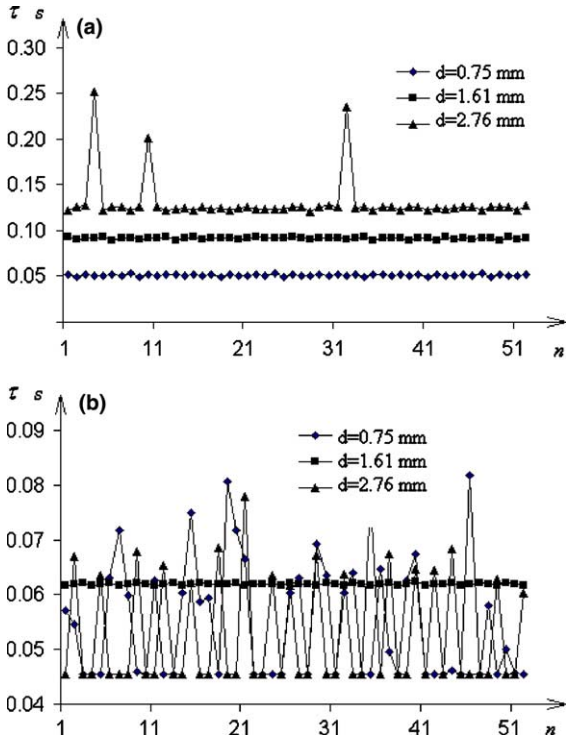

Fig. 6. Changes of time intervals versus number of bubbles n for different diameter of nozzles and volume flow rates for overpressure in the settling chamber $P = 40$ kPa: (a) $d = 0.75$ mm, $St = 0.023$, $V = 1$ l/h; $d = 1.61$ mm, $St = 0.098$, $V = 1$ l/h; $d = 2.76$ mm, $St = 0.330$, $V = 1.4$ l/h; (b) $d = 0.75$ mm, $St = 0.003$, $V = 12$ l/h; $d = 1.61$ mm, $St = 0.034$, $V = 11.2$ l/h; $d = 2.76$ mm, $St = 0.130$, $V = 12$ l/h.

identification of regions of periodic and chaotic regions is difficult.

Fig. 10 presents results of Fourier analysis of data obtained by hydrophone for nozzle 0.9 mm and shown in Fig. 4(a). Fourier analysis allows identification of bubble departure frequencies f_d and frequencies characteristic for bubble deformation after detachment. The two frequencies characteristic for bubble deformation have larger amplitude than the others. These two frequencies have been denoted by number 2 and 3. The first frequency is equal to $\approx 5/3 f_d$ and the other one is equal to $\approx 10 f_d$.

In Fig. 11 the 3D reconstruction of attractors from signal recorded by hydrophone for different volume flow rates has been presented. All attractors display chaotic character, but complexity of attractors increases with increasing volume flow rate.

Fig. 12 shows the results of calculation of dimension D_{-10} and D_{10} against the volume flow rate. The dimension D_{10} characterises the more dense part of attractors shown in Fig. 11. These parts of attractors are created by high frequencies of signal changes. Contrary to

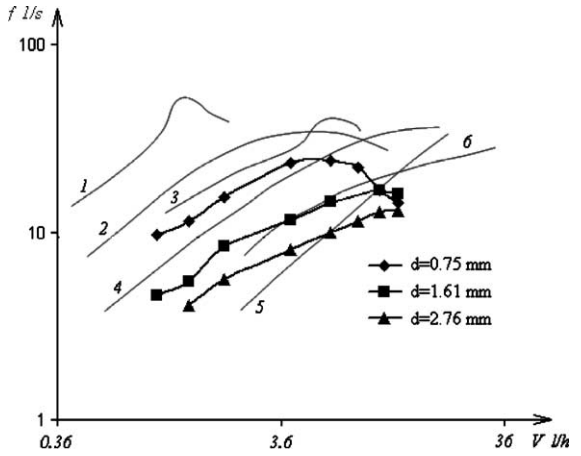

Fig. 7. Comparison of average release frequency of air bubbles obtained in the present experiment with data from literature. Curve no. 1: nozzle diameter 0.29 mm [5]; curve no. 2: nozzle diameter 0.55 mm [48]; curve no. 3: nozzle diameter 0.67 mm [5]; curve no. 4: nozzle diameter and volume of settling chamber 4 cm^3 [2]; curve no. 5: nozzle diameter 1.1 mm and volume of settling chamber 61 cm^3 [2]; curve no. 6: nozzle diameter 2.7 mm [48].

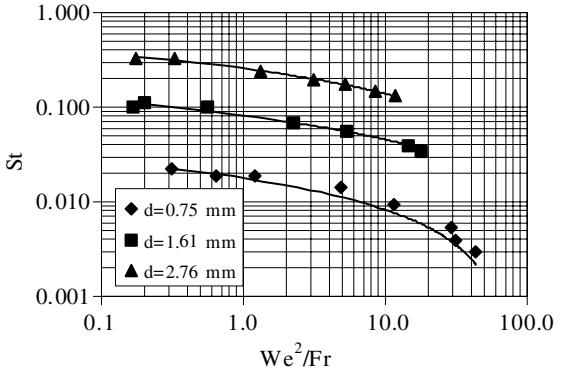

Fig. 8. Dependence of Strouhal number vs. We^2/Fr ratio for different nozzle diameter.

D_{-10} describes the less dense part of attractor which is created by process of bubble departure and its large deformation after the departure. Because D_{-10} is greater than D_{10}, so one can state, that the process of bubble deformation after departure is more complex than the process of bubble wall oscillations occurring at high frequencies. It can be concluded that multidimensional modelling of waves on bubble surface is avoidable. For high volume flow rate the wave forms on the bubble surface become more complex due to interaction between subsequent bubbles (Fig. 2).

Calculation of the largest Lyapunow exponent according to the Wolf algorithm [46,47,49] allows

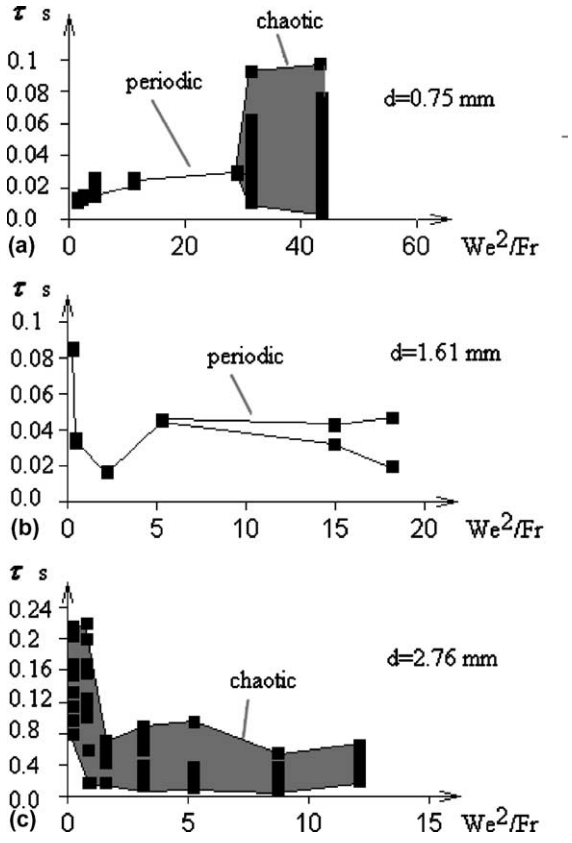

Fig. 9. Maps of chaos appearance for different diameter of glass nozzles versus We^2/Fr ratio and overpressure in the settling chamber $P = 40$ kPa.

identification the time periods for which the process of stability loss occurs. For low volume flow rate (2.5 l/h) this period corresponds to the frequency denoted as 2 in Fig. 10. With volume flow rate increase, this time period becomes over 10 times shorter.

5. Conclusions

Two different measurement techniques, i.e. laser-photodiode and an acoustic system have been applied in order to record signals generated during gas bubbles departure from a glass nozzles submerged in a distilled water.

It has been shown that this both measurement techniques developed can be used for analysis of bubble departure for low volume flow rate. In the present experiment no coalescence of subsequent bubbles has been observed for volume flow rate less than 14 l/h.

Dimensionless data presentation shows that for lower values of We^2/Fr bubble release frequency is proportional to air volume flow rate but for higher values of We^2/Fr the release frequency does not depend on the air volume flow rate.

It has been shown that bubbles dynamics is of deterministic chaos nature and behaviours of such system can be chaotic or periodic depending on the volume flow rate. It has been found that for low volume flow rate the diameter of nozzle has significant impact on bubble departure frequency and chaos appearance. Such influence was not observed for high volume flow rate. Attractor reconstruction as a result of photodiode signals analysis shows that applied measurement technique enables identification of periodic and chaotic nature of gas bubbling. In the case of chaotic nature of bubbling dimension of the attractor is much greater than for periodic bubbling.

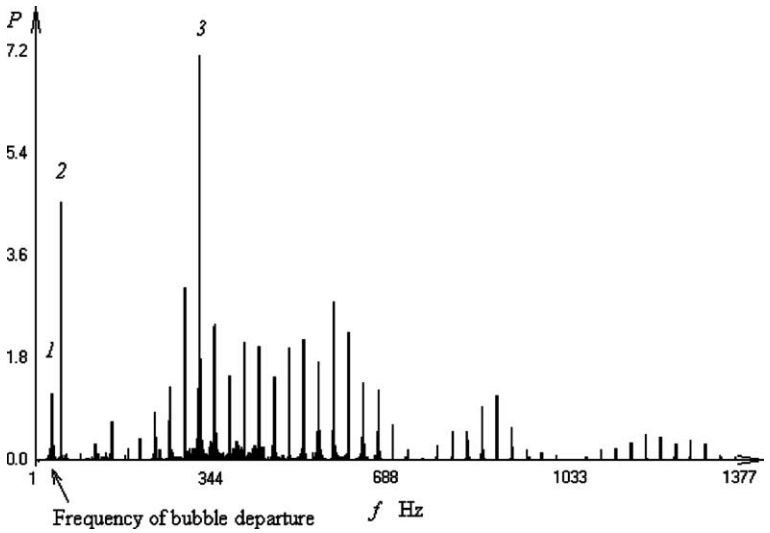

Fig. 10. Power spectrum of the signal recorded by hydrophone; fragmentary shown in Fig. 4(a).

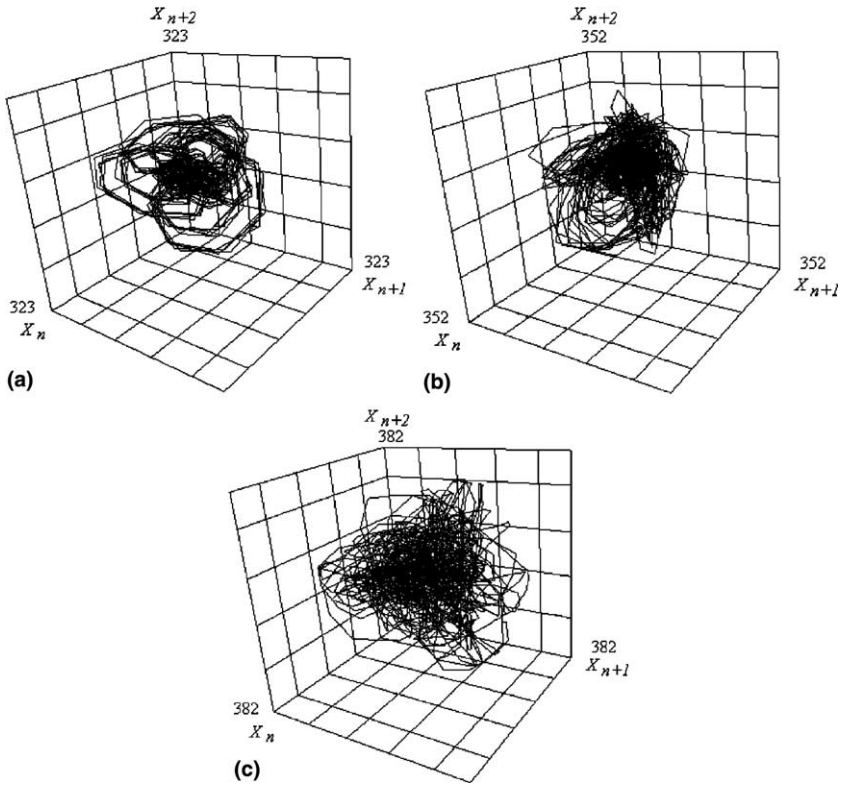

Fig. 11. 3D reconstruction of attractor for nozzle $d = 0.9$ mm, overpressure in the settling chamber $P = 10$ kPa and volume flow rates: (a) $V = 2.5$ l/h, (b) $V = 7.5$ l/h, (c) $V = 14$ l/h.

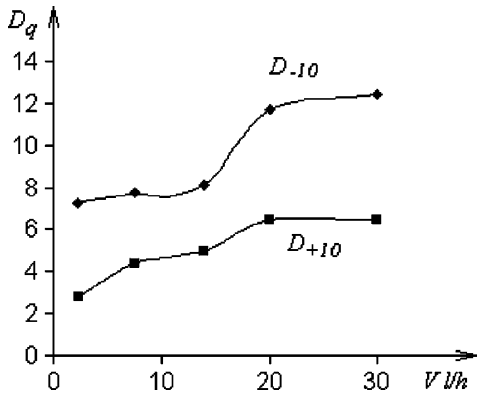

Fig. 12. Fractal dimension of data obtained by hydrophone for nozzle $d = 0.9$ mm and overpressure in the settling chamber $P = 10$ kPa.

Data recorded by acoustic system has been used for identification of bubble dynamics deformation. Obtained results revealed that the process of bubble deformation after departure is more complex than the process of high frequency oscillations of bubble wall. It suggests that waves on bubble surface can be modelled by low dimensional model.

Calculation of the largest Lyapunov exponent allows identification of the time periods in which the process of stability loss occurs. For low volume flow rate (2.5 l/h) the period in which the process of stability loss occurred corresponds with frequency $5/3f_d$ of wave on bubble wall. For high volume flow rate this time period becomes more than 10 times shorter.

References

[1] F.N. Peebles, H.J. Garber, Studies on the motion of gas bubbles in liquids, Chem. Engng. Progr. 49 (1953) 88–97.
[2] R.R. Hughes, et al., The formation of bubbles at simple orifices, Chem. Engng. Progr. 51 (1955) 557–563.
[3] L. Davidson, E. Amick, Formation of gas bubbles at horizontal orifices, AIChE J. 2 (1956) 337–342.
[4] G. Kling, Über die Dynamik der Blasenbildung beim Begasen von Flüssigkeiten unter Druck, Int. J. Heat Mass Transfer 5 (1962) 211–223.
[5] J.F. Davidson, B.O.G. Schüler, Bubble formation at an orifice in an inviscid liquid, Trans. Instn. Chem. Engrs. 38 (1960) 335–345.

[6] D.J. McCann, R.G.H. Prince, Regimes of bubbling at a submerged orifice, Chem. Engng. Sci. 26 (1971) 1505–1512.
[7] N.K. Kyriakides, E.G. Kastrinakis, S.G. Nychas, Bubbling from nozzles submerged in water: transitions between bubbling regimes, Can. J. Chem. Engng. 75 (1997) 684–691.
[8] D. Claes, Numerische Simulation von instationären Strömungen mit freien Oberflächen am Beispiel ablösender und aufsteigender Blasen. Fortschritt-Berichte VDI, Reihe 7, Nr 173, VDI Verlag, Düsseldorf, 1990.
[9] Y. Mori, K. Hijikata, L. Kuriyama, Experimental study of bubble motion in mercury with and without a magnetic field, Trans. ASME J. Heat Transfer 99 (1977) 404–410.
[10] A.L. Tassin, D.E. Nikitopoulos, Non-intrusive measurements of bubble size and velocity, Exp. Fluids 19 (1995) 121–132.
[11] P. Snabre, F.I. Magnifotcham, Formation and rise of a bubble stream in a viscous liquid, Eur. Phys. J. B 4 (1998) 369–377.
[12] W. Lauterborn, W. Hentschel, Cavitation bubble dynamics studied by high-speed photography and holography, Ultrasonics 23 (1985) 260–268.
[13] G. Grehan et al., Measurement of bubbles by Phase Doppler technique and trajectory ambiguity, in: Proceedings of the 7th International Symposium on Developments in Laser Techniques and Applications to Fluid Mechanics, Lisbon, 1994, pp. 290–302.
[14] H.S. Ko, Y.-J. Kim, Experimental analysis of bubble behaviors in circular tube, in: G.M. Carlomagno, I. Grant (Eds.), Proceedings of the 7th International Symposium on Fluid Control, Measurement and Visualization, Sorrento, Italy, 2003 [CD-ROM].
[15] V. Heinzel, A. Jianu, H. Sauter, Three-dimensional schlieren visualization of the path, shape and wake of single air bubbles rising in a stagnant fluid, in: G.M. Carlomagno, I. Grant (Eds.), Proceedings of the 7th International Symposium on Fluid Control, Measurement and Visualization, Sorrento, Italy, 2003 [CD-ROM].
[16] M.T. Stickland, W.M. Dempster, Comparison of the computed flow field around a bubble growing at an orifice using PIV techniques, in: G.P. Celata, P. Di Marco, R.K. Shah (Eds.), Proceedings of the 2nd International Symposium on Two-Phase Flow Modelling and Experimentation, Rome, 1999, Pisa: Edizioni ETS, vol. 3, 1999, pp. 1441–1448.
[17] A. Fujiwara et al., Flow structure around rising bubble measured by PIV/LIF (effect of shear rate and bubble size), in: E.E. Michaelides (Ed.), Proceedings of the ICMF-2001 (4th International Conference on Multiphase Flow, May 27–June 1, 2001, New Orleans, LA, USA), New Orleans: Tulane Univ., icmf530 [CD-ROM].
[18] J.A. Szymczyk, J.T. Cieśliński, Messung von Dampfblasengröße, Aufstiegsgeschwindigkeit und Ablösungsfrequenz beim Blasensieden mittels Particle Image Velocimetry, in: A. Delgado et al. (Eds.), Lasermethoden in der Strömungsmesstechnik—neuere Entwicklungen und Anwendungen, 8, Fachtagung, 2000, Freising, Aachen: Shaker Verlag, 2000, pp. 351–354.
[19] T.S. Leighton, The Acoustic Bubble, Academic Press, London, 1994.
[20] R. Manasseh, S. Yoshida, M. Rudman, Bubble formation processes and bubble acoustic signals, in: Proceedings of ICMF'98, Lyon, 1.2-9 [CD-ROM], 1998.
[21] R. Manasseh, T. Nicholls, Drops inside bubbles, Album of Visualization, 13, Japanese Society of Visualization, 1996.
[22] R. Manasseh, Acoustic sizing of bubbles at moderate to high bubbling rates, in: Proceedings of Experimental Heat Transfer, Fluid Mechanics and Thermodynamics, Brussel, 1997, pp. 943–947.
[23] S. Ramakrishnan, R. Kumar, N.R. Kuloor, Studies in bubble formation-I: Bubble formation under constant flow conditions, Chem. Engng. Sci. 24 (1969) 731–747.
[24] R. Clift, J.R. Grace, M.E. Weber, Bubbles, Drops and Particles, Academic Press, New York, 1978.
[25] W.V. Pinczewski, The formation and growth of bubbles at submerged orifice, Chem. Engng. Sci. 36 (1981) 405–411.
[26] F. Raymond, J.-M. Rosant, A numerical and experimental study of the terminal velocity and shape bubbles in viscous liquids, Chem. Engng. Sci. 55 (2000) 943–955.
[27] L. Zhang, M. Shoji, Aperiodic bubble formation from submerged orifice, Chem. Engng. Sci. 56 (2001) 5371–5381.
[28] T. Kumada, H. Sakashita, H. Yamagishi, Pool boiling heat transfer-I. Measurements and semi-empirical relations of detachment frequencies of coalesced bubbles, Int. J. Heat Mass Transfer 38 (1995) 969–977.
[29] M.I. Dias, R. Breit, M.L. Riethmuller, Non-intrusive measurement technique to analyze bubble formation, in: Proceedings of Experimental Heat Transfer, Fluid Mechanics and Thermodynamics, Brussel, 1997, pp. 949–956.
[30] R.P. Chhabra, Bubbles, Drops, and Particles in Non-Newtonian Fluids, CRC Press, Boca Raton, Florida, 1993, p. 164.
[31] J. Costes, C. Alran, Models for the formation of gas bubbles at a single submerged orifice in non-Newtonian fluid, Int. J. Multiphase Flow 4 (1978) 535–551.
[32] W. Luewisutthichat, A. Tsutsumi, K. Yoshida, Chaotic hydrodynamics of continuous single-bubble flow system, Chem. Engng. Sci. 52 (1997) 3685–3691.
[33] H.Z. Li, et al., Chaotic bubble coalescence in non-Newtonian fluids, Int. J. Multiphase Flow 23 (1997) 713–723.
[34] R. Femat, J.A. Ramirez, A. Soria, Chaotic flow structure in a vertical bubble column, Phys. Lett. A 248 (1998) 67–79.
[35] R. Kikuchi, et al., Diagnosis of chaotic dynamics of bubble motion in a bubble column, Chem. Engng. Sci. 52 (1997) 3741–3745.
[36] D.J. Tritton, C. Egdell, Chaotic bubbling, Phys. Fluids A 5 (1993) 503–505.
[37] K. Nguyen, et al., Spatio-temporal dynamics in a train of rising bubbles, Chem. Engng. J. 65 (1996) 191–197.
[38] M.C. Ruzicka, et al., Intermittent transition from bubbling to jetting regime in gas–liquid two phase flows, Int. J. Multiphase Flow 23 (1997) 671–682.
[39] A. Tufaile, J.C. Sartorelli, Hénon-like attractor in air bubble formation, Phys. Lett. A 275 (2000) 211–217.
[40] A. Tufaile, J.C. Sartorelli, Chaotic behavior in bubble formation dynamics, Physica A 275 (2000) 336–346.
[41] A. Tufaile, J.C. Sartorelli, The circle map dynamics in air bubble formation, Phys. Lett. A 287 (2001) 74–80.
[42] R. Mosdorf, J.T. Cieśliński, Fractal analysis of pressure changes during gas bubble emission, in: D.M. Maron

(Ed.), International Symposium on "Multiphase Flow and Transport Phenomena", Antalya, Turkey, New York, Wallingford, Begell House, 2001, pp. 70–77.

[43] J.T. Cieśliński, R. Mosdorf, Identification of chaotic attractors in gas bubbling, in: G.P. Celata, P. Di Marco, A. Goulas, A. Mariani (Eds.), Proceedings of the 5th World Conference on Experimental Heat Transfer, Fluid Mechanics and Thermodynamics, vol. 2, 2001, Thessaloniki, Pisa: Edizioni ETS 2001, pp. 1233–1236.

[44] R. Mosdorf, M. Shoji, Chaos in bubbling—nonlinear analysis and modelling, Chem. Engng. Sci. 58 (2003) 3837–3846.

[45] K. Pawelzik, H. Schouster, Generalized dimension and entropies from a measured time series, Phys. Rev. A (Rapid Communications) 35 (1) (1987) 481–483.

[46] H.G. Schuster, Deterministic Chaos, An Introduction, PWN, Warszawa, 1993 (in Polish).

[47] E. Ott, Chaos in Dynamical Systems, Cambridge University Press, Cambridge, 1993.

[48] W. Siemes, Gasblasen in Flüssigkeiten. Teil I: Entstehung von Gasblasen an nach oben gerichteten kreisförmigen Düsen, Chem. Ing. Technol. 26 (1954) 479–496.

[49] A. Wolf, J.B. Swift, H.L. Swinney, J.A. Vastano, Determining Lyapunov Exponent from a Time series, Physica D 16 (1985) 285–317.